TALLINN UNIVERSITY OF TECHNOLOGY
SCHOOL OF ENGINEERING
Department of Electrical Power Engineering and Mechatronics

CRUISING STABILITY IMPROVEMENT OF AUTONOMOUS DELIVERY ROBOT: A COMPARATIVE STUDY BETWEEN 6-WHEEL AND 4-WHEEL ROBOTS

AUTONOOMSE KOHALETOIMETAMISROBOTI STABIILSUSE PARANDAMINE: 6- JA 4-RATTALISTE ROBOTITE VÕRDLEV UURING

MASTER THESIS

Student: ..... Jung Mee Choi .....
/name/

Student code: ..... 214207 MAHM.....

..... Mahmoud Ibrahim, ...
Supervisor: ..... Early-Stage Researcher.....
/Name, position/

Tallinn, 2024

(*On the reverse side of title page*)

AUTHOR'S DECLARATION

Hereby, I declare that I have written this thesis independently.
No academic degree has been applied for based on this material. All works, major viewpoints and data of the other authors used in this thesis have been referenced.

"..13..." ....May..... 2024..

Author: ..Jung Mee Choi .....
/signature /

Thesis is in accordance with terms and requirements.

"..13..." ..May..... 2024

Supervisor: ….Mahmoud Ibrahim.....
/signature/

Accepted for defence.

"....."......May .....2024.

Chairman of theses defence commission: .....
/Name and signature/

Non-exclusive Licence for Publication and Reproduction of Graduation Thesis[1]

I, ___ Jung Mee Choi _____ (name of the author) hereby

1. grant Tallinn University of Technology (TalTech) a non-exclusive license for my thesis

_____

_____CRUISING STABILITY IMPROVEMENT OF AUTONOMOUS DELIVERY ROBOT: A COMPARATIVE STUDY BETWEEN 6-WHEEL AND 4-WHEEL ROBOTS_____,

(*title of the graduation thesis*)

supervised by _____Mahmoud Ibrahim_____,

(*Supervisor's name*)

1.1 reproduced for the purposes of preservation and electronic publication, incl. to be entered in the digital collection of TalTech library until expiry of the term of copyright;

1.2 published via the web of TalTech, incl. to be entered in the digital collection of TalTech library until expiry of the term of copyright.

1.3 I am aware that the author also retains the rights specified in clause 1 of this license.

2. I confirm that granting the non-exclusive license does not infringe third persons' intellectual property rights, the rights arising from the Personal Data Protection Act or rights arising from other legislation.

_____13 May 2024_____ (*date)*

---

1 *The non-exclusive licence is not valid during the validity of access restriction indicated in the student's application for restriction on access to the graduation thesis that has been signed by the school's dean, except in case of the university's right to reproduce the thesis for preservation purposes only. If a graduation thesis is based on the joint creative activity of two or more persons and the co-author(s) has/have not granted, by the set deadline, the student defending his/her graduation thesis consent to reproduce and publish the graduation thesis in compliance with clauses 1.1 and 1.2 of the non-exclusive licence, the non-exclusive license shall not be valid for the period.*

Department of Electrical Power Engineering and Mechtronics

THESIS TASK

Student: ……Jung Mee Choi, 214207……..(name, student code)

Study programme, ……MAHM Mechatronics…….. (code and title)

main speciality:

Supervisor(s):……Early-stage researcher, Mahmoud Ibrahim ….(position, name, phone)

Consultants: ……..(name, position)

…… (company, phone, e-mail)

Thesis topic:

(in English) CRUISING STABILITY IMPROVEMENT OF AUTONOMOUS DELIVERY ROBOT: A COMPARATIVE STUDY BETWEEN 6-WHEEL AND 4-WHEEL ROBOTS

(in Estonian) AUTONOOMSE KOHALETOIMETAMISROBOTI STABIILSUSE PARANDAMINE: 6- JA 4-RATTALISTE ROBOTITE VÕRDLEV UURING

Thesis main objectives:

1. Analysis on cruising stability of 6-wheel ADR
2. Introducing a novel design of 4-wheel ADR
3. Comparative study between 6-wheeler and 4-wheeler cruising stability

Thesis tasks and time schedule:

No	Task description	Deadline
1.	Background research and CAD modelling of ADR	Mar.2024
2.	Creating MATLAB Simulink model for simulation	Apr.2024
3.	Final compilation of thesis	May 2024

Language: …English…… **Deadline for submission of thesis:** ".13.."..May...2024

Student: …Jung Mee Choi ….....……..... "..13.."…May.....2024…a

/signature/

Supervisor: …… …….. "...13.."…….May…….2024….a

/signature/

Consultant: …… …..... "……."…….....20….a

/signature/

Head of study programme: …… ..... "……."…….....20…..a

/signature/

Terms of thesis closed defence and/or restricted access conditions to be formulated on the reverse side

CONTENTS

LIST OF ABBREVIATIONS AND SYMBOLS 7

1. INTRODUCTION 8

2. LITERATURE REVIEW 11

2.1 Rover vehicle mechanism 11

2.2 Torsional spring and motor 14

2.3 Review summary 16

3. Rover vehicle design 18

3.1 Six-wheeler with bogie mechanism 18

3.2 Four-wheeler with belly wheels 19

3.3 Suspension system 23

3.3.1 Torque limiter and worm gear 23

3.3.2 Systems for 6-wheel rover vehicle 24

3.3.3 Systems for 4-wheel rover vehicle 25

3.4 Motor selection & control 25

3.4.1 Motor selection 25

3.4.2 Motor control & sensors 26

4. Modelling and simulation 28

4.1 Governing Equations 28

4.1.1 Six-Wheeler 30

4.1.2 Quad-wheeler 31

4.2 MATLAB Simulink model 32

4.2.1 Six-Wheeler Model 32

4.2.2 Quad-Wheeler Model 38

4.2.3 Comparison and analysis 40

5. Conclusion 42

SUMMARY 43

LIST OF REFERENCES 45

LIST OF ABBREVIATIONS AND SYMBOLS

ADR – Autonomous delivery robot

BLDC – Brushless direct current

CNT – Carbon nanotube

COM – Centre of mass

IMU – Inertia measurement unit

LMD – Last mile delivery

PID – Proportion-Integral-Differential

1. INTRODUCTION

The rapid development of AI-driven autonomous driving and machine vision technology has expanded the ability to provide delivery services using autonomous delivery robot vehicles. An autonomous delivery robot (ADR) is suitable for the last mile delivery (LMD) which handles local delivery of small packages with varying delivery order frequencies and high-volume [1]. Due to their size and low cruising speed, ADRs are more suitable to be operated on pedestrian sidewalks [2]. According to a study [3], LMD market size is predicted to grow from 5,31 billion USD in 2024 to 29,13 billion USD in 2032.

Autonomous driving technology involves versatile environmental perception which requires robot vehicles to perceive surroundings using cameras, active radar, ultrasonic sensors, integrated navigation etc. followed by spatial referencing called localisation and sophisticated control. Two main approaches are dominating the market. One is camera based and the other is lidar based. Both approaches involve intensive multi-sensor fusion schemes including radar and ultrasonic sensor systems [4]. Nevertheless, camera-based technology is considered a more economical solution demanding less hardware resources and space, thus suitable for small vehicles. Currently, ADR applications for LMD have achieved level 3 of driving automation where the vehicle handles most cruising tasks but requires the operator's assistance in complex or unexpected situations [5].

The delivery robot encounters many challenges while operating on the pedestrian sidewalk such as traffic light crossings, obstacle detection & avoidance, yielding paths to pedestrians and other vehicles, climbing curbs, etc. Many different types of robots are introduced to perform such tasks in the market. Among many, a 6-wheel-based vehicle is considered versatile due to its capability to climb curbs and low obstacles. Such ability is endowed from the bogie mechanism where 2 wheels are articulated with a single rod when viewed from a side. When the actuator(motor) attached to the centre of the rod rotates, it elevates the front part of the body to climb an obstacle with a certain height of up to i.e. 15 cm. To pair as a bogie mechanism, either 2 front wheels or 2 rear wheels are combined, and the remaining wheel is only engaged for driving as shown in Figure 1.1.

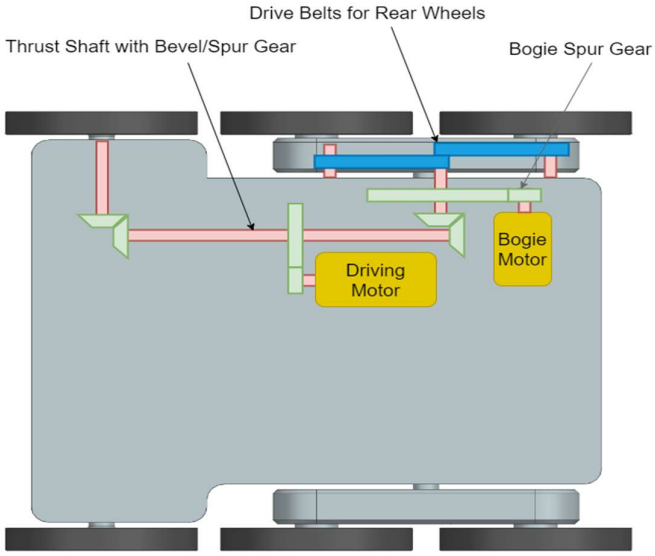

Figure 1.1. General mechanism scheme of 6-wheel ADR (Top half view) – Rear wheel combined

Nevertheless, such outstanding feature has its disadvantages due to 2-wheel axes mutually dependent to each other by a bogie mechanism. Unintended turning of the bogie motor happens constantly by diverse ground conditions making the wheel suspension system more susceptible to distortion. Moreover, cruising acceleration will add torque to a bogie hinge causing vehicle's pitching movement. Presence of a physical hinge makes rotation more distinctive compared with a rigid chassis. All these factors result in deteriorating not only the cruising stability and behaviour but also unstable ground contact of wheels. Unstable ground contact limits or reduces gradability of the vehicle (steep hill cruising) and turn-in-place ability (180° turn).

Another aspect is the stable and smooth turning of the vehicle. Instead of a steering mechanism, the 6-wheel ADR performs differential steering to turn direction, which functions well during cruising. However, viewed from the top, a rectangular formation of wheels makes it hard for the vehicle to turn in place (180° turn) causing more tyre abrasion due to friction. So, it is efficient to lift two rear wheels so that the remaining 4 wheels form a near-square formation to make smooth turning on a circular trajectory. Nevertheless, it is still challenging to make a smooth turn on irregular surfaces such as unpaved roads or on inclined surfaces such as sidewalk ramps or hills.

ADR during mission encounters countless challenges and problems that require remote operating assistance. In manual mode, the robot vehicle receives numerous and continuous command signals given by the human operator which tends to be more vigorous than in autonomous driving mode since the engagement of the human operator means the robot is in a place or a situation where AI driving algorithm is unable to resolve the encountered problem. Controllability of the vehicle should be simple and

effective to react promptly to escape from the troubled situation amid communication latency between the operation centre and the robot. Whether it is computer or human, it requires extra efforts to control a 6-wheeler with bogie mechanism.

Conclusively, poor cruising stability and ground contact are induced by:

- Pitching movement induced by acceleration.
- Uneven ground surface or sloped area
- Poor suspension system.

Lack of shock absorbing ability also causes frequent and constant vibration on onboard electronics such as cameras, sensors, graphic card, storage devices, communication modules, etc. making the ADR more prone to operational failure.

In this study, the improvement of the 6-wheel bogie mechanism design by installing linear and torsional spring is presented and discussed. Furthermore, a novel design concept of a 4-wheeler without a bogie mechanism is introduced and analysed in comparison with the 6-wheeler. There are a total of 6 wheels in the new design but only 4 wheels are engaged with motors and in contact with the ground, and 2 wheels in roller type are installed on the bottom side of the lower chassis. These belly rollers play crucial roles when ADR climbs the curb.

The CAD models for both designs are created, and modelling & simulation of the suspension systems using MATLAB Simulink are performed and compared. The simulation results show that the novel design of the 4-wheeler outperforms the 6-wheeler. Finally, a novel methodology of curb-climbing feature of a quad-wheeler is presented and demonstrated using Siemens Motion Animation tool.

Keywords: Autonomous delivery robot, 4-wheeler, 6-wheeler, curb-climbing rover vehicle, Bogie mechanism, torsional suspension, torsional spring damper system, MATLAB Simulink, Siemens NX motion.

2. LITERATURE REVIEW

For 6-wheel robot vehicles, a lot of research is targeted for military purposes and planetary rovers that operate on rough terrain. They are equipped with a steering mechanism or with a differential joint that enables the body to rotate. Only a few of them covered the model without steering and with a bogie mechanism.

On the other hand, DC motor and torsion spring combined systems are found in study fields related to exoskeleton or biomechanical devices. Therefore, insights are gathered from different fields and combined. Accordingly, the literature review is divided into 2 sections to review the bogie mechanism part and the DC motor-torsion spring part.

2.1 Rover vehicle mechanism

Multiple studies have covered the mechanical structure of rover vehicles including bogie mechanism of 6-wheel robots.

Dongmok Kim et al. [6] focused on optimizing the link parameters of the 6-wheel-based rocker-bogie mechanism using the Taguchi method to improve climbing capability against different types of stairs minimizing undesired backward movement. The rocker-bogie mechanism has a differential joint connected to the main body which enables the body to rotate to maintain a horizontal level. Another pivot joint is connected between the rocker and the bogie to give more flexibility to the bogie mechanism.

The theory is based on the premise that a smooth trajectory of the centre of mass of the vehicle contributes a lot to the smooth climbing of stairs. The key is to maintain the centre of mass as straight as possible within the kinematic constraints. Calculations are done to define kinematic parameters and constraints, then optimization is researched via a systematic design approach, the Taguchi method. Signal to noise (S/N) ratio is analysed to evaluate chosen link parameters' quality. The higher the SN noise, the better the optimisation performance.

Hongqiang Zhao et al. [7] studied differential steering control for 6x6 in-wheel motors to drive wheels independently without steering and bogie mechanism. Non-linear gain recursive sliding mode is used to realize dynamic surface adaptive control of the trajectory tracking. Based on the dynamic model of the mobile robot, the Trucksim model is created.

Taking the torque and the direction signals as input, the model outputs longitudinal & lateral speed, yaw rate, vertical force, and wheel speed. The Trucksim model also considers non-linearity from longitudinal & lateral movement and angle changes of wheel & camber. The study implemented the dynamic surface adaptive control method using Trucksim software and Simulink to improve the steering accuracy and tracking speed.

Jaewon Nah et al. [8] researched the torque distribution problem of the skid-steered 6-wheel vehicle to improve lateral stability and manoeuvrability. The control layers are divided into 3 - upper level, lower level, and estimation layer. Longitudinal net force and yaw moment are controlled by the upper level, whereas the lower-level controls driving and braking torques. Vehicle speed, slip ratio, and tyre load data are inputs from the estimation layer. The goal is to design a driving controller that could give torque commands to each wheel to minimize longitudinal net force allocation error using Truck Sim and MATLAB Simulink.

The simulation result is compared with the 4 WD vehicle of a similar size when making a U-turn movement. Curve trajectory, yaw rate, wheel torque, lateral acceleration, and vehicle velocity are analysed, which shows better performance than conventional 4 WD vehicles but accurate speed estimation of the vehicle is crucial to predict slip ratio and friction circle estimation.

Atul Kumar Gupta et al. [9] proposed a novel design of a semi-circular rocker mechanism for a 6-wheel multi-terrain robot for multi-terrain. With a semi-circular rocker and bogie mechanism, the robot has better load transmission from the front to the rear when the front wheel collides with an object while keeping the structure more robust. The pivoting joint location on the rocker is optimized to balance between stair climbing and shock absorbing.

Maximum motor torque requirement is calculated based on which total force is derived. Dynamic simulation using ADAMS software is implemented over stairs and inclined terrains. Contact torques between front/middle/rear wheels and ground are analysed respectively. No comparison data with the conventional bar-type rocker is provided.

The paper also presented a comparison chart of previously conducted studies on 6-wheel-based terrain robots as shown in Table 2.1.

Table 2.1 Comparison of previously executed research for terrain robots

	Shrimp	Talon	Packbot	CoMoRAT
No. of motors	8	4	4	4
No. of wheels	6	6+ track belt	6+dual track belt	4+ track belt
Dimensions (mm)	639x428x278	864x572x472	686x406x178	300x500x80
Weight (Kgf)	5.4	52	10.89	-
Payload (Kgf)	3	12-45	-	15
Max. speed (m/s)	0.35	2.3	2.6	1
Turning mechanism	Front and rear wheel	Caterpillar	Caterpillar	Caterpillar
No. of motor in turning mechanism	2	0	0	0
Capability	Stair climbing	All terrain robot	All terrain robot	-
Maneuverability	4	4	4	4
Suspension	Self-adaptive	No	No	No

Zhen Song et al. [10] introduced a portable 6-wheel mobile robot with a reconfigurable body and self-adaptable climbing mechanism. The robot is designed to have a 3-rocker-leg structure and adaptive climbing rocker legs to enhance terrain adaptability and obstacle climbing ability. The bot is also foldable to improve portability and twistable for it has a Sarrus-variant mechanism in the middle of the body.

For modelling, a rotation matrix coordinate frame is established, the centre of mass, and geometric constraints are defined. Based on these, static forces for obstacle crossing in different phases are calculated to retrieve feasible regions of the angle variant which is one of the main performance parameters for the robot's huddle leaping capability together with the friction coefficient. Numerical simulation for static capability is tested to study motion stability and geometric & static passing capability. A physical prototype is also built to verify the design concept and the simulation model.

Vahid Tavoosi et al. [11] researched vertical dynamics modelling of a 6-wheel military UGV. The vehicle has a suspension arm connected to a shoulder joint for each wheel, which enables the chassis to change its height. With each wheel and hinged joint being independent, the robot can climb over a barrier or an obstacle.

The study is intended for vibrational motion in both linear and non-linear models. Each model has 5 DOF – 3 DOF in angular motion of the suspension arm, and a single DOF each for pitch angle & a vertical displacement of the vehicle body. Kane Dynamic method is used for the non-linear model of multi-body systems. 5 equations are derived which should be solved numerically. For the linear model, the Lagrange modelling method is used under a similar assumption. Simulation results for linear and non-linear models are performed with the sensitivity analysis, longitudinal velocity effect, initial angle

effect of the suspension arms, vehicle mass effect, torsional stiffness effect of the spring, and the angular damping effect.

2.2 Torsional spring and motor

Studies related to torsional spring and motor (actuator) were conducted.

Juan et al. [12] studied a general analytical model of spiral torsional springs with the strip thickness. The study found the main design parameters such as spiral curvature, length, housing structure, strip thickness bending stiffness variation along the length. An experiment was carried out to validate the model and a parametric study based on the validated model. The study concluded that the strip thickness is the most important parameter which affects the torque-turn angle characteristics.

Brian T. Knox et al. [13] researched a unidirectional series-elastic actuator (SEA) system for an experimental biped prototype using spiral torsion spring and DC motor - Torsion spring as a compliant component and DC motor as a high-stiffness actuator.

A thin wide rectangular strip of metal spring wound in to form a cylindrical shape is introduced with important design variables, followed by the mechanism design. The experiment is carried out using a prototype of 2-legged robot with 4 joints and 4 motors. The study concludes that spiral torsion springs show better operating properties over helical torsion springs in general with less connection backlash. The study focuses on the novel design of high-strength spiral torsional spring, material, and performance.

Stefano Rossi et al. [14] presented a study of a wearable robotic device that could help cerebral palsy patients' rehabilitation. Based on the prototype wearable device for ankle and knee, spring stiffness is estimated by kinematic analysis simulation varying the spring stiffness (between 1 and 4 Nm/rad) and the optimal value is identified.

To verify the mechanical characterization, a test bench is created with direct and inverse kinematics whose dynamics are evaluated by Jacobian JA, ankle-knee torque, and force. The test bed is to experiment with the control of the spring deflection from the sinusoidal signal and output torque at the joint.

The outcome of the position tracking for deflection of spring is less than 2°. The torque signal distortion is also considered because of the non-linearity of the spring and the servo-motor performance. The motor specification and the combined effect with the spring system are not fully presented.

Wilian M. dos Santos et al. [15] studied the series elastic actuator (SEA) based active orthosis. The mechanism is made of a DC motor, worm gear, and a customized torsion spring. FEA of the elastic element is performed to define design parameters such as spring constant, equivalent inertia, and damping coefficient. Then motor specification is

decided accordingly to fulfil the angular velocity of the knee joint to be around 50 rpm with a maximum torque of around 15 Nm. The reduction ratio of the worm gear is 150:1 which provides maximum continuous torque of 27.15 Nm.

The customised torsion spring with new topology is used as an elastic element. Chromium-vanadium-based steel is used to comply with the specification. FEM stress analysis is performed using ANSYS® software to verify maximum stress is within the yield strength range. The study follows with a controller design, dynamic model, and the torque & impedance control. Torque and impedance controller serves fluent interaction with the patient's movement whose performance is evaluated by frequency response analysis.

Jinyong Ju et al. [16] researched the elastic torsional vibration control of a flexible joint robot based on the mechanism method. Electromechanical coupling dynamics are modelled with a DC motor & reducer, 2 joints, and torsion spring. Then equivalent moment of inertia, armature voltage, angular velocity, and the drive torque of the DC motor are calculated. MATLAB Simulink is used to identify the parameters of the system. Through this model, spring stiffness, damping constant, and friction constant are determined. The fussy PID control method is applied as a control algorithm which can narrow between control accuracy and dynamic quality. The basic domain of the fuzzy set consists of the deviation ranges, change rate, and increments of PID coefficients.

Finally, the system is simulated and verified by experiment. The study focuses on the torsional vibration of the flexible joint transmission links using a fussy PID controller. The control methodology is effective and highly performed, however, the viable frequency range is not discussed.

Domenico Campolo et al. [17] researched the possibility of wing flapping motion using a DC motor and torsion spring at high frequency. The DC motor drives flapping wings at resonance by using an elastic mechanism, not a slider-crank mechanism. A bug-sized flyer is to hover at a flapping frequency range of 20 ~ 40 Hz with a wing stroke angle of around 60°.

Simplified non-linear damping of the wing aerodynamic model is studied to analyse the quasi-sinusoidal regime. This is to exploit spring to resonate with the wing inertia at a specific frequency. After the motor selection based on impedance matching, 2 different setups, one with inertial loading and the other with aerodynamic loading, are used to define the materials and geometry of the wing. Simulation is implemented in MATLAB environment and verified with the first setup.

Bharat Joshi et al. [18] studied a general PWM-regulated brushed DC motor model using optical incremental encoder feedback. The speed of the DC motor is based on the following mathematical model.

$$N = K\frac{(V - l_a R_a)}{Z\phi}$$

$$K = \frac{60A}{P}$$

where

$R_a = armature\ circuit\ resistance$

$I_a = armaturecurrent$

$V = motorinputvoltage$

$\phi = totalfluxofthemachine$

$Z = impedenceofthemotor$

The incremental optical encoder that can provide equally spaced pulses for linear motion generates and feed digital outputs of motor behaviour.

To sophisticatedly control the motor speed, accurate tuning of the PID controller is proposed with an incremental encoder feedback mechanism that involves quadrature phase decoding of signals and decoded position data to obtain DC motor velocity.

DC motor model is created with Simulink for parameter estimation through which non-linear least square matching parameters are obtained. The feedback system in the closed loop will obtain a PWM signal to be applied to the H-bridge to actuate the DC motor based on the PWN duty cycle. The PID controller is tuned to respond to the load change of the motor.

2.3 Review summary

Reviewing prominent articles convinces that stabilizing the bogie mechanism intended for smooth turning and preventing pitching requires combined and extended study from different articles mentioned in this chapter. Also, the majority of research is focused on military and multi-terrain purposes, topology and the mechanism tend to be more expensive and complicated with suspension arms in-wheel motors, steering mechanism, etc.

Therefore, it is necessary to implement research on the stability of a 6-wheel-based bogie mechanism for urban purposes with a simpler mechanism and control algorithm to evade or overcome obstacles on pedestrian ways and crossings. MATLAB Simulink

and optimization methodology are powerful tools for modelling and simulation widely used in research.

The study aims to apply a mechanical torsional spring on the pivoting hinge of the bogie to absorb shocks from the ground and recover from any distortion while the DC motor will apply a certain amount of torque to suppress pitching induced by acceleration. When the robot is in a static state, a well-responding torsion spring will be responsive to ground surface irregularity or on a ramp, and the bogie DC motor can react to adjust minor gaps to improve the ground contact.

3. ROVER VEHICLE DESIGN

In this chapter, ADR vehicle designs are discussed, and CAD models are presented. Due to limited design information available from the commercial operators, only the overall chassis model of the 6-wheeler is presented based on the opened source [2]. However, the novel design of the 4-wheeler is created in detail and the inner structure with electromechanical components are presented.

3.1 Six-wheeler with bogie mechanism

The main purpose of using 6 wheels is to feature a curb climbing function using a bogie mechanism. Front wheels and rear wheels are divided depending on the bogie combination. As The study model has one front wheel and two rear wheels when viewed from the side.

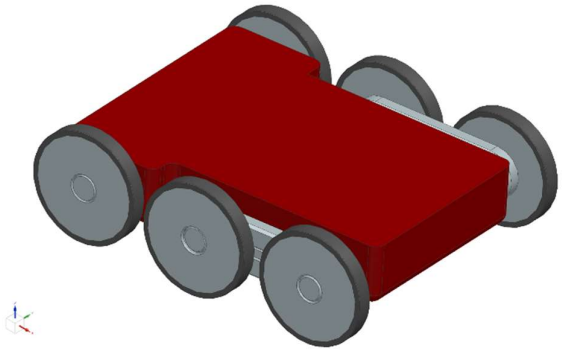

Figure 3.1. ISO view of 6-wheeler chassis

A pivoting point is located at the centre of bogie mechanism bar between two rear wheels that rotates up and down as shown in Figure 3.2.

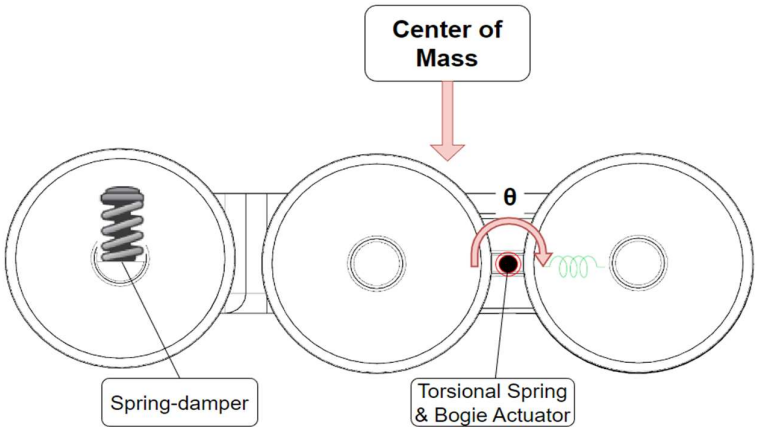

Figure 3.2 Side view of 6-wheeler chassis

Figure 3.3 shows how bogie mechanism activates.

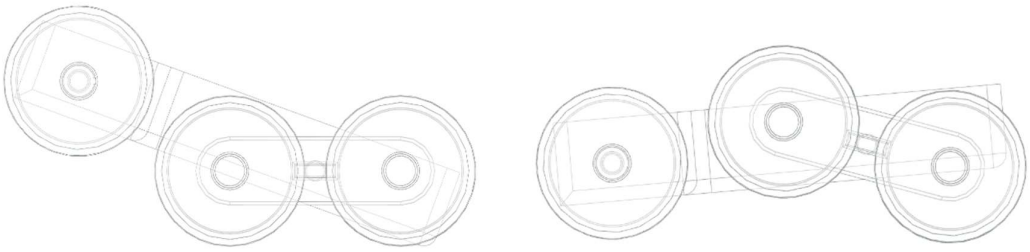

Figure 3.3. Bogie mechanism upward(A) and downward(B)

Bogie-down position triggers the nose-up posture of the vehicle which enables the curb-climbing function. Climbing curbs using a bogie mechanism is not always successful. The curb height is not the only factor but also payload, ground surface angle, tyre grip against the curb affects successful climbing.

The bogie-up position decreases the vehicle mass distribution point from 6 to 4, thus enhancing ground contact. This position is useful when cruising on a slopped area or even on snowy roads.

Advantages of 6-wheeler with bogie mechanism are:

- Stability due to the low COM and the body sustained by 6 wheels.
- Curb climbing capability (approximate height less than or equal to 15 cm)

Disadvantages are:

- Unstable ground contact due to the bogie mechanism articulating two wheels and the absence of an individual suspension mechanism.
- Difficult to install suspension system – insufficient space due to wheels positioned too close to each other and the presence of a bogie mechanism.

3.2 Four-wheeler with belly wheels

A novel design concept is introduced to overcome the disadvantages of a 6-wheeler with a bogie mechanism. A new design also has a total of 6 wheels, but the appearance resembles a 4-wheeler. Two roller-type belly wheels are attached to the bottom of the chassis which play a crucial role when climbing curbs and serve as safety wheels to protect the chassis in case of any wheel leg failure.

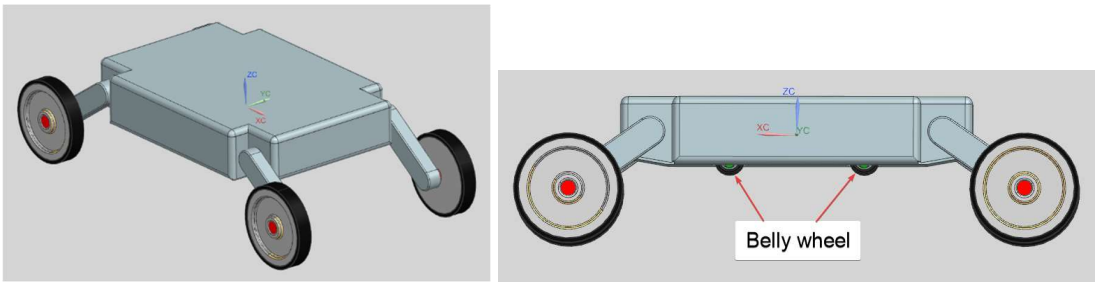

(A) (B)

Figure 3.4 ISO view (A) and side view (B) of 4-wheeler

There are 2 BLDC motors for cruising – one for the left and the other for the right. The cruising motor transmits torque through the bevel gear shaft. Power transmission divided into left and right enables differential steering and turn-in-place ability of the robot. The inner mechanism is shown in Figure 3.6 and Figure 3.6.

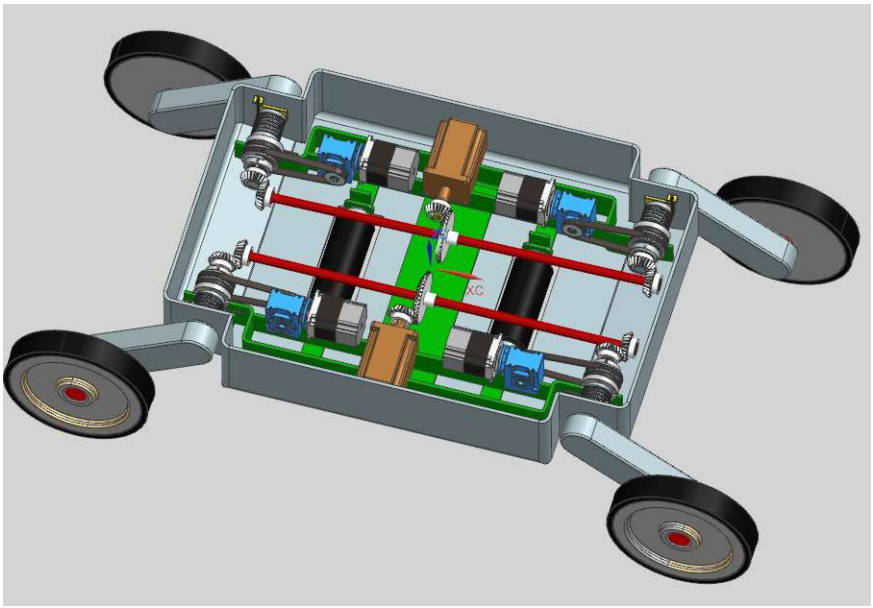

Figure 3.5 ISO view of inner mechanism layout.

The vehicle chassis has a symmetric structure in widthwise and lengthwise. 4 identical wheel mechanism is installed on each joint. 2 driving BLDC motors are in the middle transmitting power through the bevel gears and the drive shaft. Each wheel leg can be raised independently using the DC servo motor. Wheel leg motor is connected to a worm gear with a reduction ratio of 10:1, and the drivebelt connects power transmission between the gear and the torque limiter. The torque limiter protects the motor and driving mechanism from unintended torque transmitted from the wheel. A torsional spring is installed on the wheel leg shaft to act as a shock absorber. Driving power is transmitted through the hallow shaft and to the wheel by a driving belt.

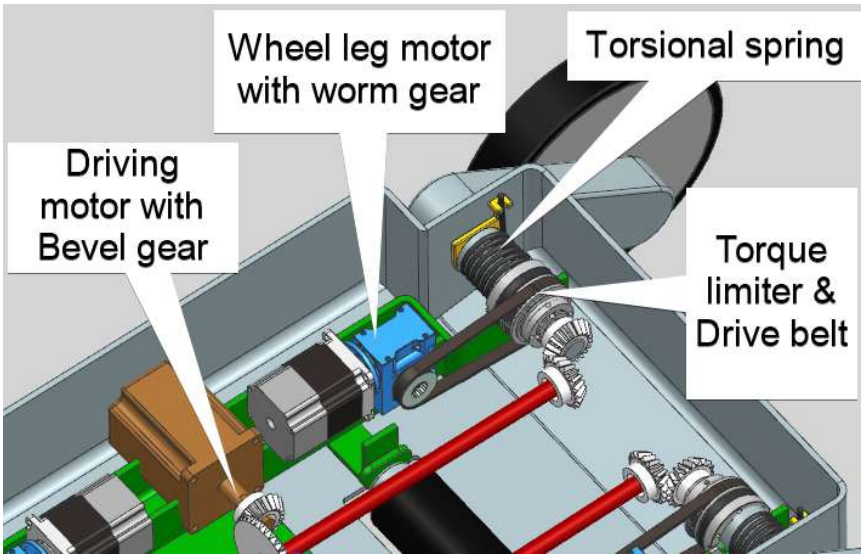

Figure 3.6 Major components of 4-wheeler inner mechanism.

Unlike most 4-wheel rover vehicles, the novel design is capable of climbing curbs. Since the 4-wheeler cannot elevate 2 front wheels simultaneously, it must climb curbs by sequentially elevating her front wheel legs one by one and sliding with belly wheels. Demonstration of the curb climbing feature is presented in

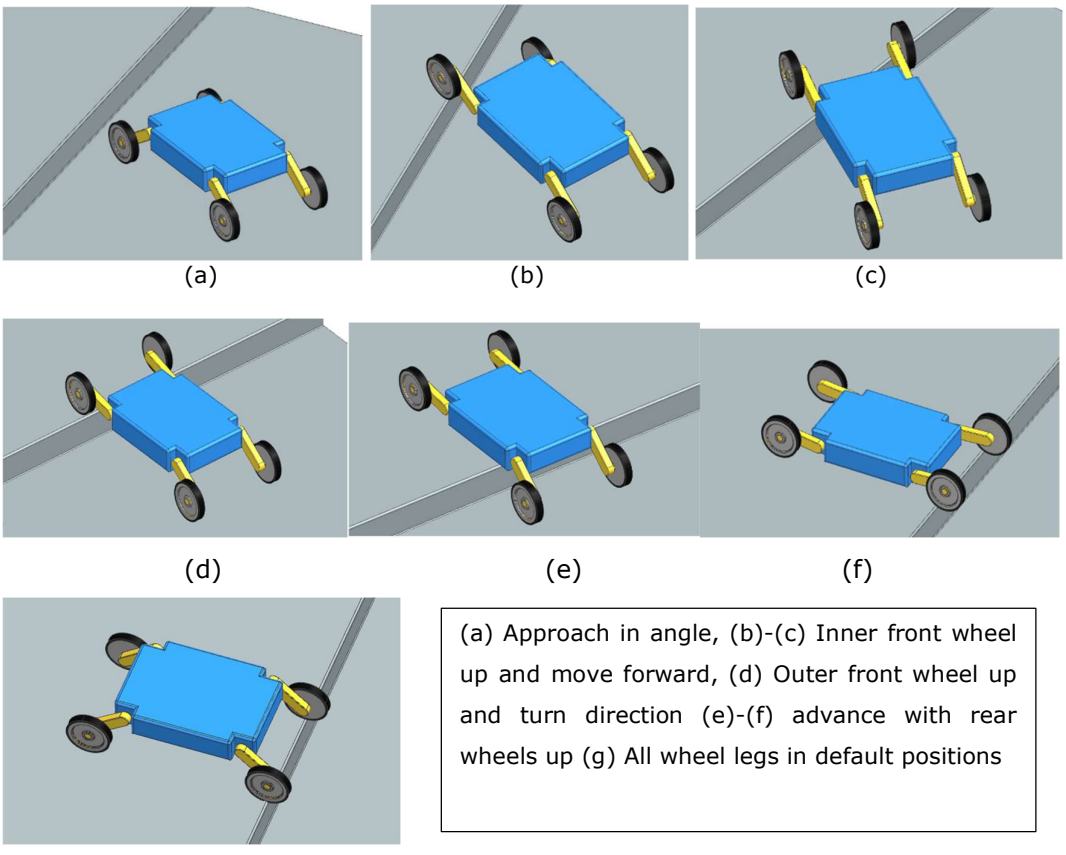

(a) Approach in angle, (b)-(c) Inner front wheel up and move forward, (d) Outer front wheel up and turn direction (e)-(f) advance with rear wheels up (g) All wheel legs in default positions

Figure 3.7 Demonstration of curb climbing process.

When a wheel leg is lifted, it is safer to adjust vehicle's COM to the opposite side of the raised wheel leg to prevent the robot collapsing diagonally to the ground. COM can be shifted to the left or right by changing the wheel leg angle. Side view of above step (f) and (g) are shown in Figure 3.8.

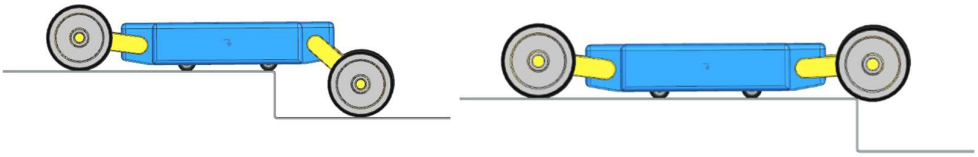

Figure 3.8 Side view of 4-wheeler executing curb climbing.

The belly rollers can be passive or active depending on the degree of wheel grip. To minimize the motor installation, passive wheels can be an economical option but active wheels with motor engagement will enhance the curb climbing performance.
The curb climbing process algorithm is depicted in Figure 3.9.

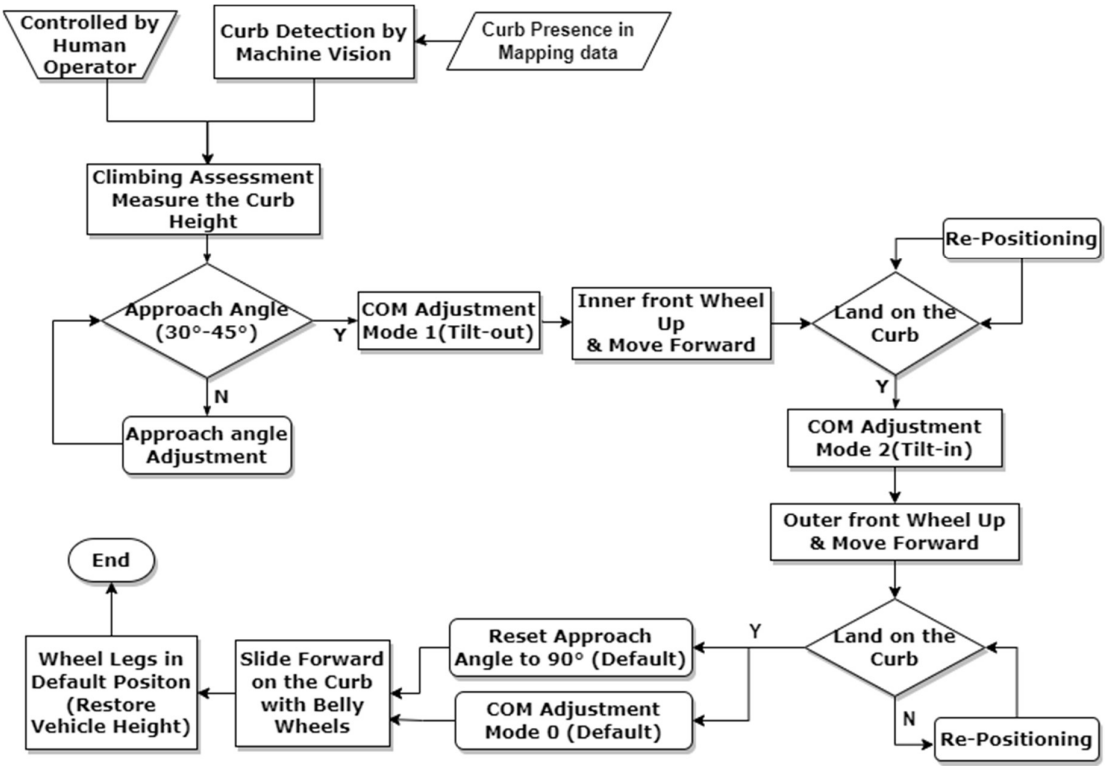

Figure 3.9 Curb climbing process flowchart for 4-wheeler.

3.3 Suspension system

Most ADR do not have suspension systems since comfort is not a prioritized consideration in design. However, the minimum suspension system will contribute to enhancing cruising stability, ground contact, and prolonging product lifetime by protecting electric & mechanical components sensitive to shocks and vibrations.
Considering the small overall size of ADR with limited space in the chassis, a simple compact system is considered in the study.

3.3.1 Torque limiter and worm gear

The study assumes a torsional spring damper system applicable to both 6-wheeler and 4-wheeler – at bogie hinge for 6-wheeler and at wheel leg hinge for 4-wheeler.
The torsional suspension mechanism requires:

- external torque induced by the ground disturbance is not to be transmitted to the drive belt-motor system for protection purposes.
- servo motor should be able to transmit torque to control wheel leg rotation.

Torque limiter

Suitable damping device should be considered with the torsional spring. Torsional damper is quite bulky and costly to install in a small size vehicle. Rubbery damper so called a vibration eliminator has hub shaft surrounded by an inertial ring where rubber is filled in between [19]. The structure is simple and economical, but the device is designed to reduce constant rotational vibration along a shaft axis and prevent resonance. Above all, its angular range is too small for this application.
Although limited, torque limiter can satisfy both requirements for this application. The main role of the torque limiter is to protect the motor mechanism by slipping unintended external rotations transmitted from the ground. This feature is crucial when motor is engaged with a rotary-type suspension system. The motor must exert intended torque to change the wheel leg angle, but it should not be affected or harmed by the external torque induced by the ground obstacles.
There are mainly 2 types of torque limiter - friction based and magnetic field based. Friction based torque limiter – with a ball detent mechanism will be considered in this study because of its advantage of low cost, lightweight and good torque-to-weight ratio. However, this type is more prone to mechanical wear and not suitable for continuous slip application [20].

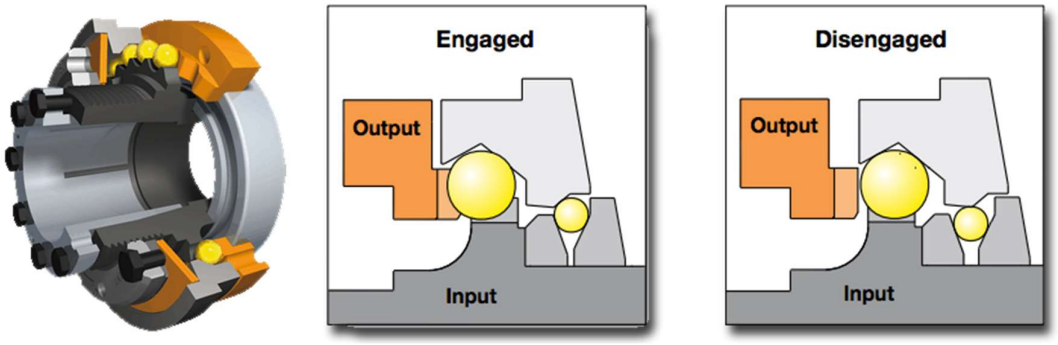

(A) (B)

Figure 3.10 Ball detent torque limiter (a) and engaging mechanism (B) [21]

In addition to the original purpose of limiting torque, it can behave as a torsional damper because it is based on mechanical friction to slip unintended load transferred. Coulomb friction damping theory can be applied for analysis and modelling.

Hall effect sensor or electromagnetic rotation sensor will be installed at the hub hinge of the wheel leg joint, hence exact rotational position of the wheel leg is detected and feedback to the motor controller.

Worm gear

Worm gear offers a large reduction ratio with anti-reversing feature, which does not allow worm wheel to drive a worm unless specially designed for that purpose. This kinematic characteristic perfectly serves the second purpose of the suspension system. Motor can control the wheel leg rotation, but the opposite way is mechanically locked. External torque will be dissipated by the torque limiter because of the anti-reversing nature of a worm gear. On the other hand, it is possible for the motor to rotate the wheel leg withing the torsional spring displacement range and the torque limiter set value. Therefore, a mechanical combination of torque limiter and a worm gear set satisfies all conditions required for the wheel leg suspension system as shown in Figure 3.6.

3.3.2 Systems for 6-wheel rover vehicle

It is obvious that the bogie mechanism must be responsive to various cruising conditions and environments to enable smooth driving while maintaining a certain degree of manoeuvrability. Therefore, to improve the 6-wheel ADR design, the following criteria is considered.

- Reserve the conventional chassis model curtailing massive design revision.
- Implement modification within the limited space in the chassis.

- Minimize the improvement cost of both design and manufacturing.

To accomplish the above goals, a bogie mechanism consisting of a torsional spring and DC motor is considered. DC motor(actuator) is already presented in the existing designs but adding a torsional spring requires the motor to counteract with the mechanical spring system. The bogie motor can also be designed to compensate the marginal displacement gap uncovered by the mechanical spring.
6-wheeler chassis has limited space since it must accommodate 6 wheels and relevant driving mechanism. Therefore, a small cantilever spring-damper system can be an option for the front wheel suspensions. Rear wheels require a different approach due to the presence of a bogie mechanism. A bogie bar that connects two wheels makes the torsional spring the only economical option without a damper. A vertical spring-damper system will make the mechanism more expensive and complicated.

3.3.3 Systems for 4-wheel rover vehicle

For quad-wheelers with wheel legs, all wheel suspensions can have an identical type. Whether it's torsional or cantilever-type spring-damper system, leaf-type springs, or torsion bar types, they will provide easier design, installation, and tuning the system compare with 6-wheeler. 4 identical torsional springs are used in the study.
In general, torsional spring performs nonlinearly within the entire operational angle, that is, the higher the bending angle, the stiffer the spring is. However, it can be assumed linear if the bending angle is small. testing alternative spring types such as etc.

3.4 Motor selection & control

This section discusses motor selection and control methodology focused on 4-wheeler. Cruising motor is excluded but only wheel leg control motors are studied. Motor selection can be applied to 6-wheeler bogie mechanism as well. Motors and sensors play great role in establishing AI-based control strategies.

3.4.1 Motor selection

AC induction motor is a prominent solution for many industrial scale applications including automotives. However, for small size vehicle with relatively low cruising speed such as ADR, DC motor is more suitable because it makes the system lighter by omitting the inverter to transfer DC to AC. Therefore, the following DC motors are compared for the motor selection.

Table 3.1. DC motor comparison for ADR [22], [23], [24]

DC Motor Type	Advantage	Disadvantage	Remarks
Brushed DC Motor	Simple speed and torque control	Noise, wear-out, regular maintenance	Speed is controlled by the applied voltage
BLDC Motor	Electrical commutator-abrasion free	complex control circuitry needs continuous monitoring of the rotor position	Position: Hall effect sensor/speed: PWM duty cycle
Servo motor	Load-responsive, high efficiency and accuracy, maintains constant torque in a wide speed range and is less noisy than stepper motor	Higher cost, hard to tune the controller, heat must be dissipated in the higher speed range	Suitable for industrial robots and automation
Stepper motor	Low cost, constant holding torque, Simple control especially in an open loop, longer life	No compensation for missed step Torque decreases as speed escalates Noisier than servo motor	No position feedback Suitable for constant load application

A brushless DC (BLDC) motor has an electrical characteristic similar to a DC motor, but its configuration is similar to a permanent magnet synchronous AC motor. Instead of mechanical commutation, electric commutation results in reducing maintenance of the motor [25], making BLDC more suitable for cruising and driving. In this study, BLDC motor is used for a driving motor and a DC servo motor to control bogie and wheel legs.

3.4.2 Motor control & sensors

Wheel leg motor controls the posture of the robot vehicle body - rolling and pitching. If all four wheels are engaged, the overall vehicle body height is adjustable (maximum height equals the length of the wheel leg). This makes is when the ADR can make turn in place movement to change the cruising direction exactly opposite.

The exact posture information of the robot is given by the inertial measurement unit (IMU) sensor, which is crucial to control the rolling and pitching of the chassis body. This is especially important when the robot vehicle performs curb-climbing task. The 4-wheeler must elevate one wheel leg up where imbalance takes place. Lowering the opposite side of wheel legs shifts the COM away from the unbalanced point preventing the robot from collapsing.

Ultrasonic sensors and cameras are typical sensors to detect obstacles to prevent collisions. This short-range sensor is very effective to detect solid objects nearby and measure distance to the object. Camera images are also useful to train neural network-based AI object detection and improving curb-climbing algorithms.

Despite main material being rubber, modern tyres which contain carbon nanotube (CNT) are electrically conductive to release static electricity from tyre to the ground [26]. Ground contact sensor can be applied to detect the exact ground contact of each wheel. Using this principle, continuity tester-based grounding sensor can detect whether wheel is in good contact with the ground or not. Based on this data, bogie and wheel leg motors can be further adjusted accurately to ensure ground contact of all wheels. Nevertheless, it is still a challenge to achieve the desired level of electrical conductivity while maintaining the sound mechanical properties of the tyre, because the uniform conductivity is accomplished by a sophisticated control of dispersion and distribution of CNTs within the rubber matrix [27].

4. MODELLING AND SIMULATION

The simulations are performed in this chapter to compare cruising stability. Suspension systems of the vehicles are modeled and simulated using MATLAB Simulink. Modelling and simulation of both 6-wheeler and quad-wheeler vehicles are studied for comparison. Suspension system dynamics are modeled based on torsional spring suspension types and equivalent motions of equations.

The suspension system of a passenger vehicle focuses on passenger comfort and there are many affecting parameters as follows: [28]

- Road surface conditions
- Aerodynamic forces
- Vibrations from engine and driveline
- Design quality of wheel assembly and tyre.

However, this study excludes factors irrelevant to ADR such as aerodynamics and complex wheel assembly. Also, aerodynamic impact is negligible since ADR has relatively small size. Therefore, the road height and the force induced by acceleration are inputs and the vertical displacement and angular pitching of the vehicle are outputs. A general modelling scheme is shown in Figure 4.1.

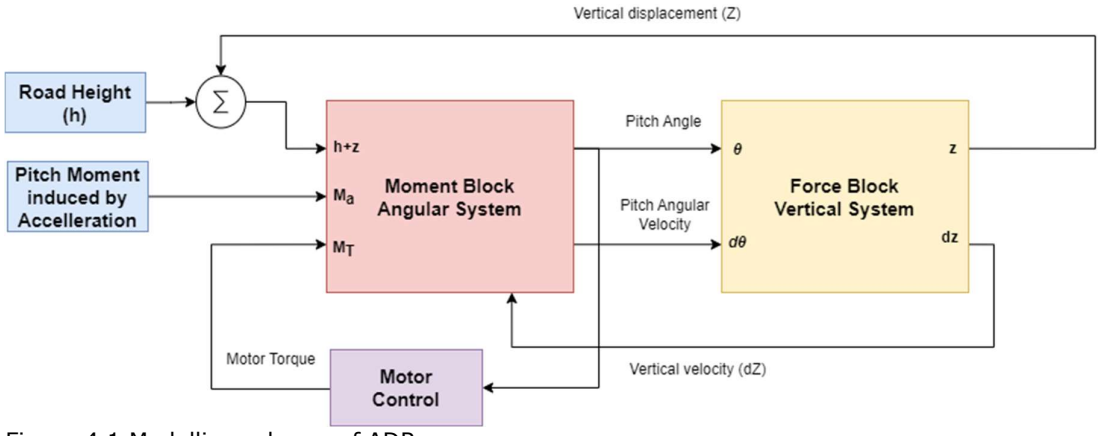

Figure 4.1 Modelling scheme of ADR

Motor control block is an option feature since the study focuses on harmonic vibration of torsional spring-damper system. However, a simple PID controller and an application of reverse torque are studied to observe any further improvements.

4.1 Governing Equations

Equations of motions are established to mathematically model system dynamics. Two sets of 2^{nd} order ordinary differential equations – one for force and the other for

momentum are obtained. A free body diagrams (FBD) of 2 models are presented in each relevant section. Some assumptions are made for simplicity. Approximation is applied for small angles.

$$Z = L \cdot sin\theta$$
$$Z \approx L \cdot \theta \ (if\ \theta\ is\ small)$$

The rotational moment of inertia of the vehicle is calculated using the parallel axis theorem, so called Steiner's theorem [29] [30] [31]. It is defined as

$$I = I_{cm} + md^2$$

$where$

$I: moment\ of\ inertia\ on\ random\ axis$

$I_{cm}: moment\ of\ inertia\ about\ the\ mass\ centre$

$m: body\ mass$

$d: distance\ from\ the\ axis\ to\ the\ mass\ centre$

According to this, pivoting point for moment inertia is shifted to a bogie hinge - a parallel movement by l_r and a lateral movement by l_h.

$$Iyy = \frac{1}{12}(M_b) * (L_v^2 + H_v^2) + (M_b \cdot l_r^2) + (M_b \cdot l_h^2)$$

Where

$M_b: Vehicle\ body\ mass$

$L_v: Vehicle\ length$

$H_v: Vehicle\ height$

$l_r: Length\ between\ COM\ and\ bogie\ hinge$

$l_h: Height\ between\ COM\ and\ bogie\ hinge$

Torsional spring constant and damping coefficient are defined in torque equation as

$$T = k_t \cdot \theta$$

$where$

$T: torque\ (Nm)$

$k_t: torsional\ spring\ constant\ \left(\frac{Nm}{rad}\right),$

$\theta: angular\ displacement\ (rad)$

$$T = c_t \cdot \dot{\theta}$$

$where$

$c_t: torsional\ damping\ coefficient\ \left(\frac{N.m.s}{rad}\right),$

$\dot{\theta}: angular\ velocity\ \left(\frac{rad}{s}\right)$

Translational spring constant can be used.

$$F = k_z \cdot z$$

$$= k_t \left(\frac{\omega}{l \cdot \cos \omega}\right) \left[\frac{Nm}{rad}\right]\left[\frac{rad}{m}\right]$$

$$k_z = k_t \left(\frac{\omega}{z \cdot l \cdot cos\ \omega}\right)$$

For the translational damping coefficient,

$$F = c_z \cdot v$$

$$= c_t \left(\frac{\dot{\omega}}{l}\right) \left[\frac{Nms}{rad}\right]\left[\frac{rad}{s}\right]\left[\frac{1}{m}\right]$$

$$c_z = c_t \cdot \frac{\dot{\omega}}{\dot{z}} \cdot \frac{1}{l}$$

4.1.1 Six-Wheeler

Half-car suspension system is modelled as shown in Figure 4.2. All 6-wheels share equal amount of normal force and acceleration force.

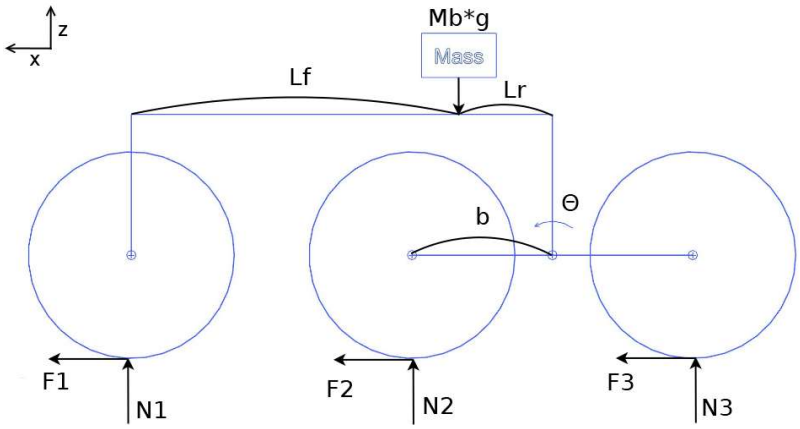

Figure 4.2 Freebody diagram of 6-wheeler chassis.

Two key assumptions are considered in this model. First, the COM should be designed to be positioned slightly rear side of the vehicle, so that when curb climbing feature is activated by the bogie mechanism, the front wheels are elevated. Another important consideration is the pivoting point of pitching movement. Normal automotive model that has a rigid body does not have a physical hinge for pitching, so pitching happens with respect to the COM of the vehicle. However, for 6-wheeler, pitching does not take place at the COM but rather at the bogie motor hinge due to the presence of physical hinge. Therefore, the pitching point of the vehicle body is offset from COM to the centre of the bogie, thus the pitching angle is equal to the rotating angle of the bogie.

Governing Equations

$$m\ddot{z} = k_f(L\theta - (h + z)) + c_f\left(L\dot{\theta} - \dot{z}\right) - mg \quad [Force]$$

$$I_{yy}\ddot{\theta} = M_A + M_f - T_M - C_t\dot{\theta} - k_t(\theta - \theta_h) \quad [Moment]$$

where

m: Body mass

θ: Pitch angle

z: Vertical displacement

L: Moment arm (bogie bar)

h: Road height

k_f: Spring constant (front)

c_f: Damping coefficient (front)

Iyy: Moment of inertia

M_a: Moment induced by acceleration,

M_f: Front wheel moment,

T_M : Motor torque,

c_t: Damping coefficient,

k_t: Torsional spring constant,

θ_h: h angle

The translated angle from the bogie arm and the road height is calculated as:

$$\theta_h = \sin\left(\frac{h}{b}\right)$$

4.1.2 Quad-wheeler

4-wheeler requires different approach from 6-wheeler. Instead of a half-car suspension, a quarter-car model suffices because of all identical symmetric suspension system structure. Nevertheless, the wheel legs are stretched out from the vehicle body, Model needs to be separated by the sprung and unsprung mass. Sprung mass is the vehicle main body and unsprung mass is the wheel and wheel leg. Figure 4.3 shows the free body diagram of a quarter-car model for 4-wheeler.

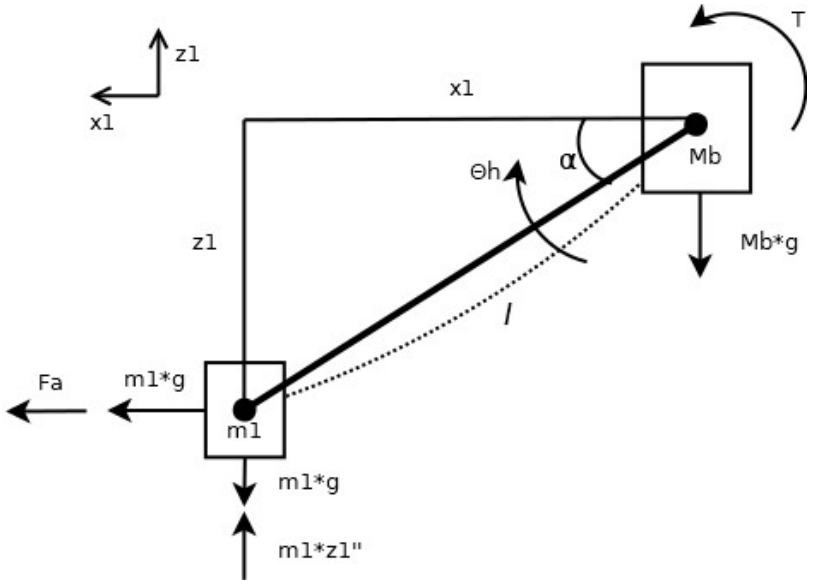

Figure 4.3 Free body diagram of a quarter-car model for 4-wheeler.

Torque from the torsional spring-damper (T) is resisting force from the wheel (m_1). Road step (h) is transformed to an angular form (Θ_h) resulting an angular displacement

(α). A vertical and horizontal displacements (z_1 and x_1) change with respect to angular displacement which can be represented as follow.

$$T = K_t\alpha + C_t\ddot{\alpha}$$

$$x_1 = l \cdot \cos\alpha$$

$$z_1 = l \cdot \sin\alpha$$

Using the above and forming the governing equations:

$$I_{yy}\ddot{\alpha} = (m_1\ddot{z_1} - m_1 g)x_1 + m_1\ddot{x_1}z_1 + F_a + T - T_h$$

where

I_{yy}: $A\ moment\ of\ inertia\ of\ the\ wheel\ \&\ wheel\ leg\ body$

T_h: $torque\ induced\ by\ the\ road\ height\ h\ (Kt\theta_h + C_t\ddot{\theta_h})$

$$m\ddot{z} = m_1\ddot{z_1} - (m_1 + m_b)g$$

4.2 MATLAB Simulink model

To validate the cruising stability and performance, simulation models are created using MATLAB Simulink for both 6-wheeler and 4-wheeler. Common simulation conditions are applied to both 6-wheeler and 4-wheeler.

- Simulation time is 20s
- Acceleration starts at t=2
- Step input (h=0.05m) is given at t=10.

4.2.1 Six-Wheeler Model

Based on the governing equations, Simulink blocks are formed to solve differential equations of the suspension system. Top hierarchy block diagram model is shown in Figure 4.4.

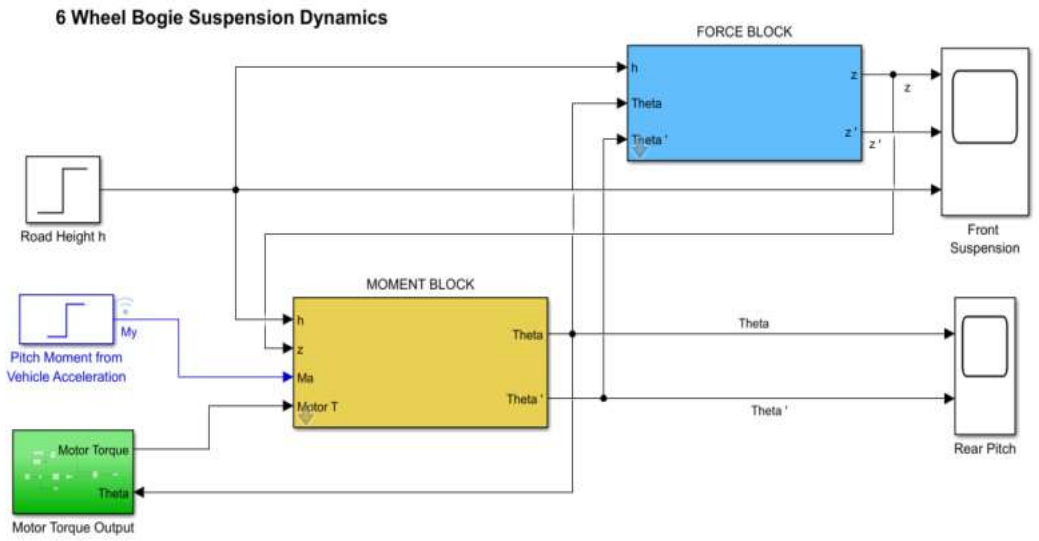

Figure 4.4 General block diagram of the suspension dynamics model.

The road height and the vehicle acceleration are two external inputs. The force block calculates vertical elements, and the moment block calculates pitching angle and angular velocity. Figure 4.5 shows the detailed calculation block diagrams.

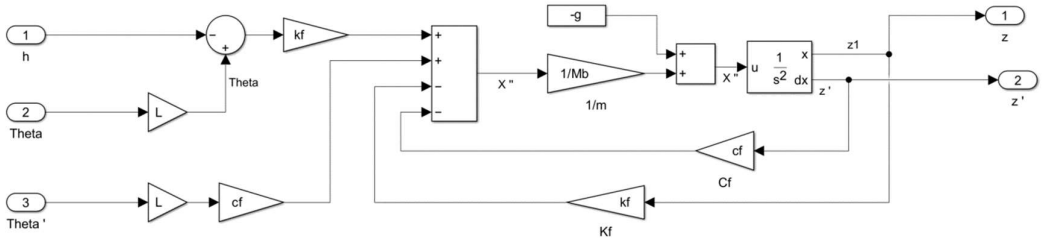

(a)

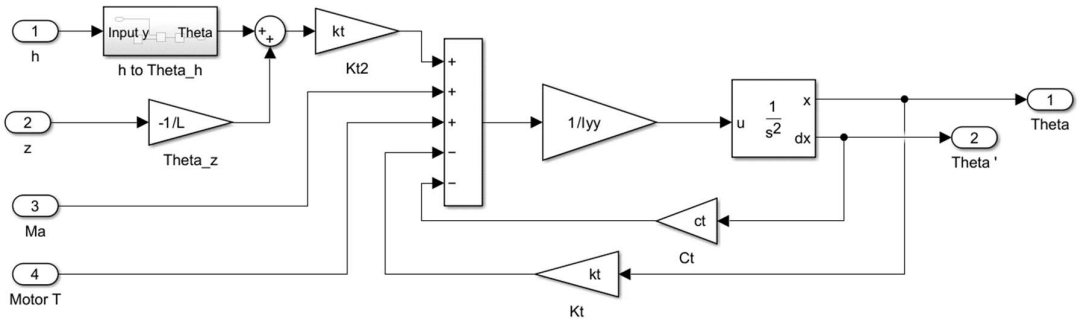

(b)

Figure 4.5 .(a) Force block,(b)Momentum block.

For 6-wheelers, the existing model which doesn't have suspension systems is presented first followed by models with properly tunned suspension systems.

Simulation results

Simulation results are depicted in 3 groups.

- Without suspension
- Suspension without reverse torque
- Suspension with reverse torque.

Displacement and velocity of the vertical and angular response are presented.

As shown in Figure 4.6, it is obvious that the system without suspension shows extremely unstable fluctuation with countless secondary ripples in displacement curve and the velocity curve is out of acceptable range.

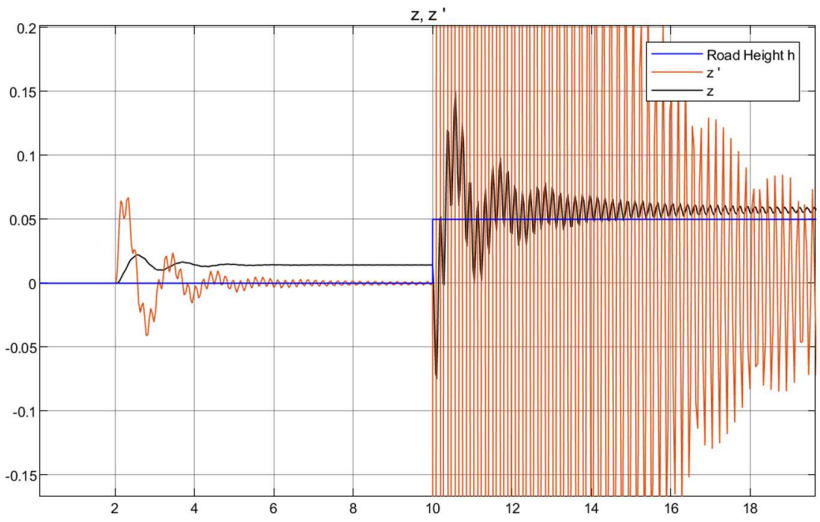

Figure 4.6 Vertical response without suspension.

Applying proper suspension gives more stable response as shown in Figure 4.7. Although the curve converges and, the system is unable to narrow the z curve to the road height (h).

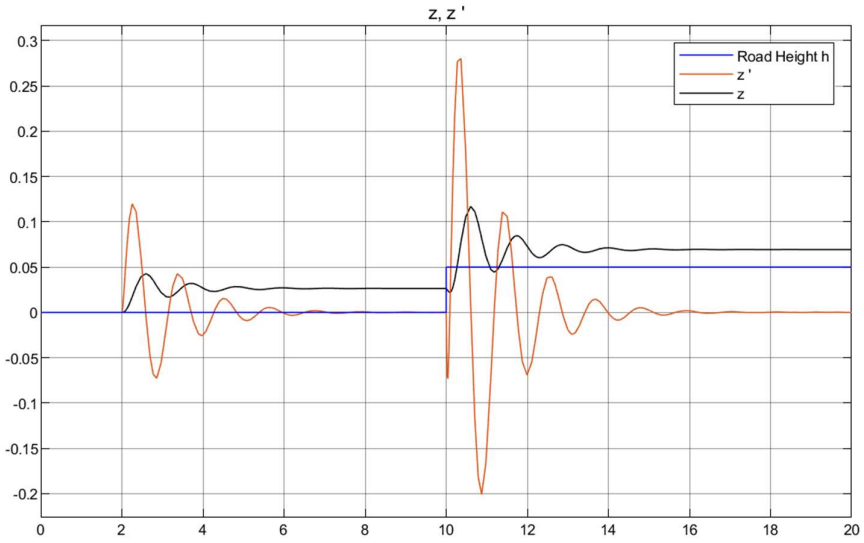

Figure 4.7 Vertical response with suspension.

It's mainly due to a pitching moment induced by acceleration. The pitching angle concerning the bogie hinge of the vehicle is shown in Figure 4.8. The pitching angle starts around 3.8° during acceleration and reaches over 17° after hitting the road height.

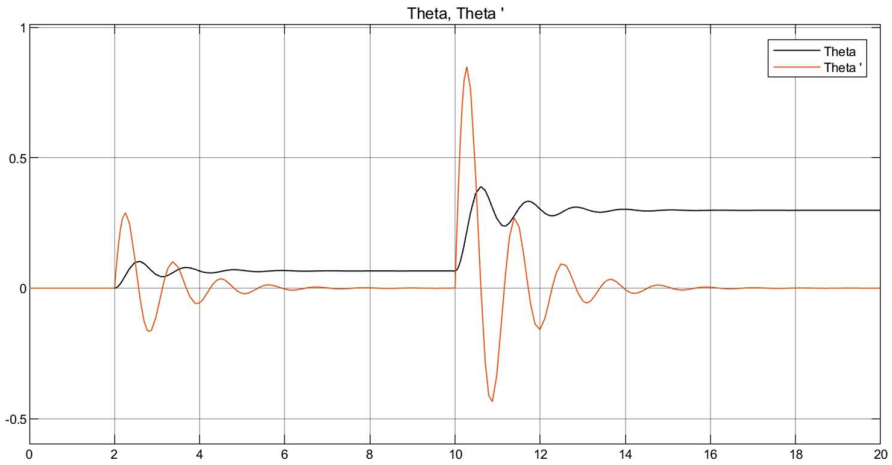

Figure 4.8 Pitching response.

Therefore, the bogie motor can engage to suppress the pitching moment by applying reverse torque. As shown in Figure 4.9 and Figure 4.10, both vertical and angular displacements are reduced.

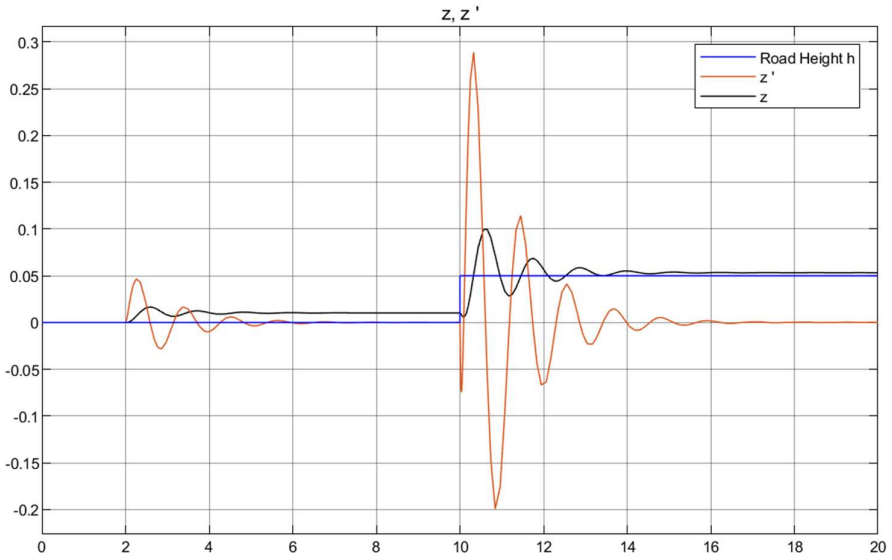

Figure 4.9 Vertical response with suspension & reverse torque

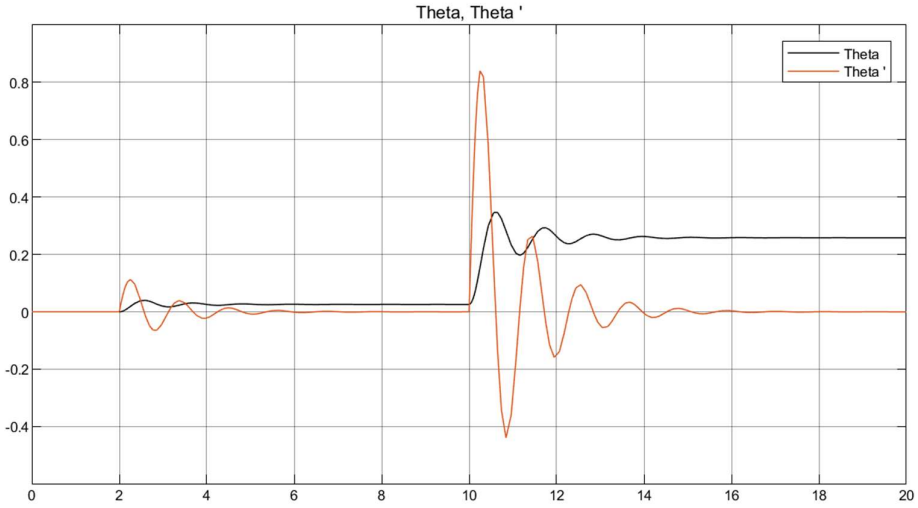

Figure 4.10 Pitching response with suspension & reverse torque

Important improvements are elaborated in tables.

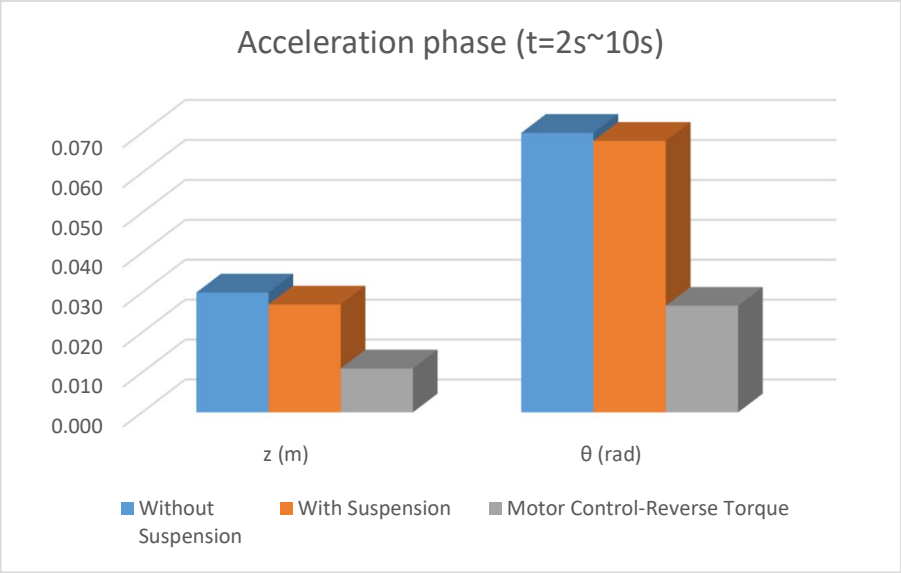

Figure 4.11 Comparison during acceleration phase (6-wheeler)

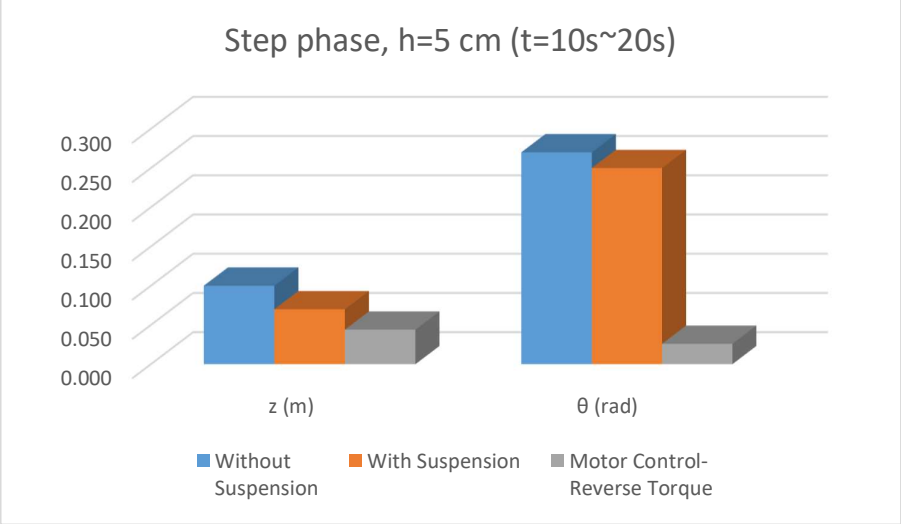

Figure 4.12 Comparison during step phase (6-wheeler)

There isn't significant overall difference in both vertical and pitching movement between with suspension system and without suspension system, but the distinct differences is the stability of the curves. As shown in Figure 4.6, severe fluctuations in displacement curve means the vehicle is vulnerable to external vibration.

Reverse torque definitely improves the system response but only during acceleration phase and a single step-obstacle phase. Above all, the reverse torque value is preset and calculated according to the initial acceleration and the road height. In a real cruising

environment, this is unpredictable. The suspension system itself must be resilient to absorb heterogenous vibrant external disturbances.

4.2.2 Quad-Wheeler Model

In a quarter-car suspension system with torsional spring-damper, angular displacement *α* is the key parameter. Figure 4.13 shows Simulink block diagram of a quarter-car suspension model for the 4-wheeler.

Input parameters such as step size & time and acceleration value are as same as the 6-wheeler model for comparison analysis. The momentum block calculates rotational angle of the hinge where torsional spring-damper is installed. The angular displacement is feedforwarded to both horizontal and vertical displacement blocks to convert angular to translational displacement.

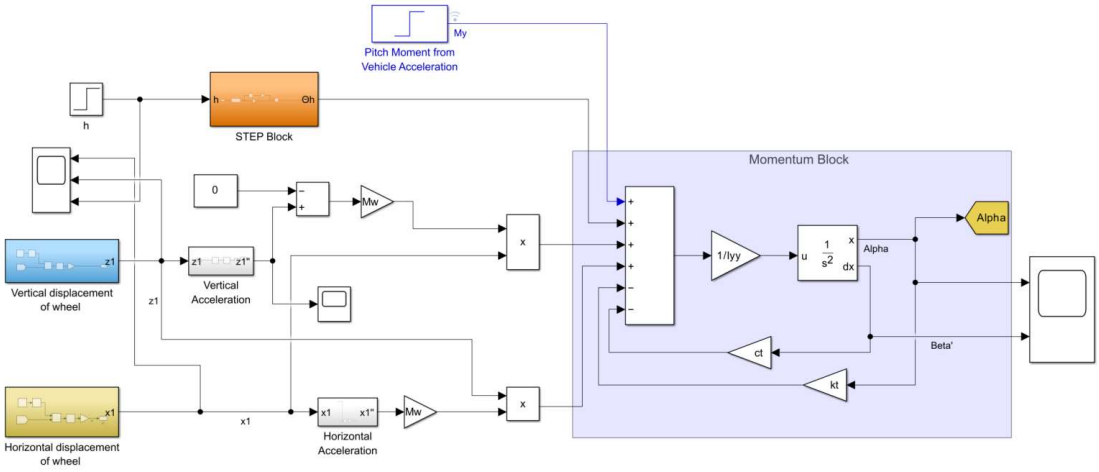

Figure 4.13 Block diagram of quarter-car model of 4-wheeler suspension

Unlike 6-wheeler model, motor torque control block is unnecessary because 4 -wheeler having 4 independent suspension system is expected to return stable response, and these result will be compared with 6-wheeler's results.

Simulation results

As shown in Figure 4.14, angular response of the suspension system is very stable.

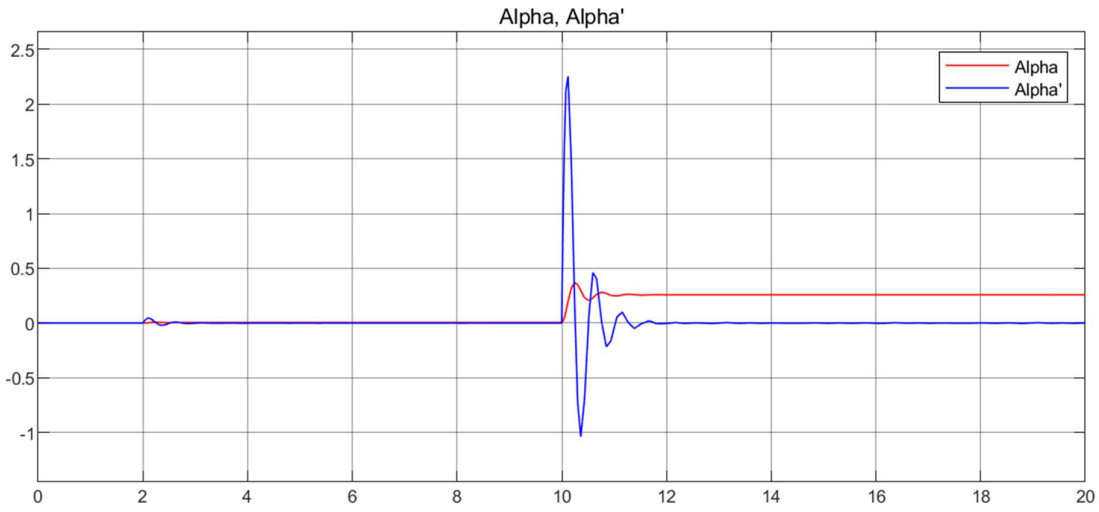

Figure 4.14 Angular response of 4-wheeler quarter-car model

Only a minimal fluctuation at the beginning of acceleration phase is observed, which diminishes quickly. Also, during the step phase, overshooting is minimized and converges softly to the road height (*h*) in a second. Such behaviour is also observed in the translational response shown in Figure 4.15.

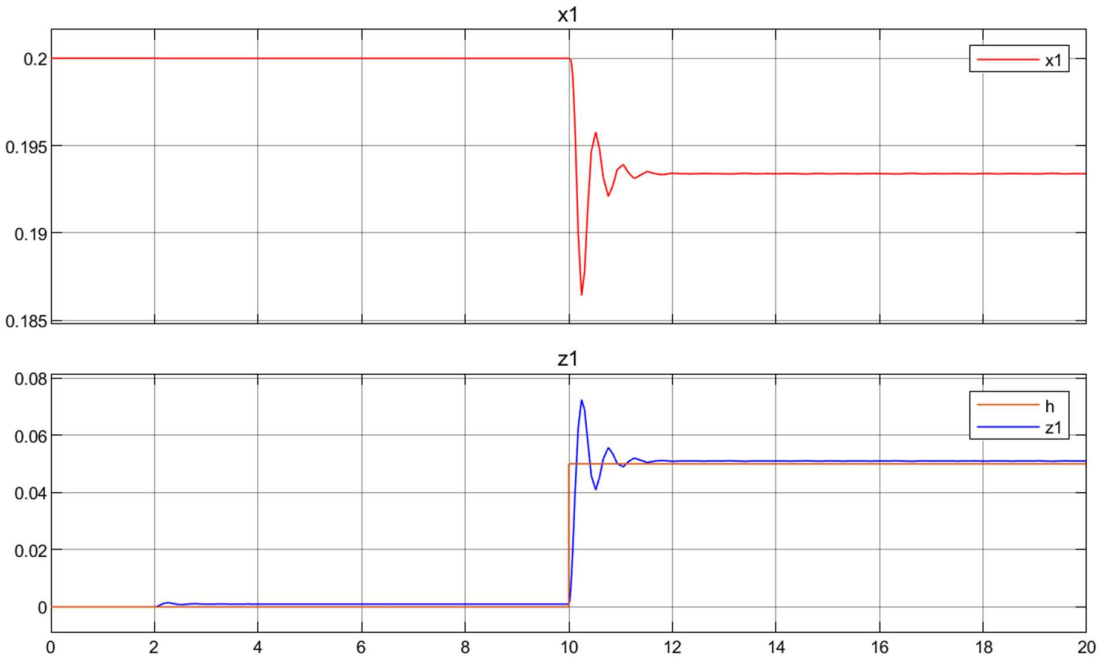

Figure 4.15 Translational response of 4-wheeler quarter-car model

4.2.3 Comparison and analysis

System response of both 6-wheeler and 4-wheeler is compared. For 6-wheeler, 2 results (suspension with and without reverse torque) are selected to compare with 4-wheeler suspension without reverse motor torque.

Comparison during acceleration phase is shown in Figure 4.16. It is obvious that 4-wheeler's performance in terms of both vertical and angular displacement is superior to those of 6 wheelers. Pitching movement induced by acceleration for 4-wheeler is almost zero and angular displacement 80% lower than that of 6-wheeler suspension with reverse torque. This implies that 4-wheeler without a controller can cruise with superior stability than 6-wheeler with a motor controller.

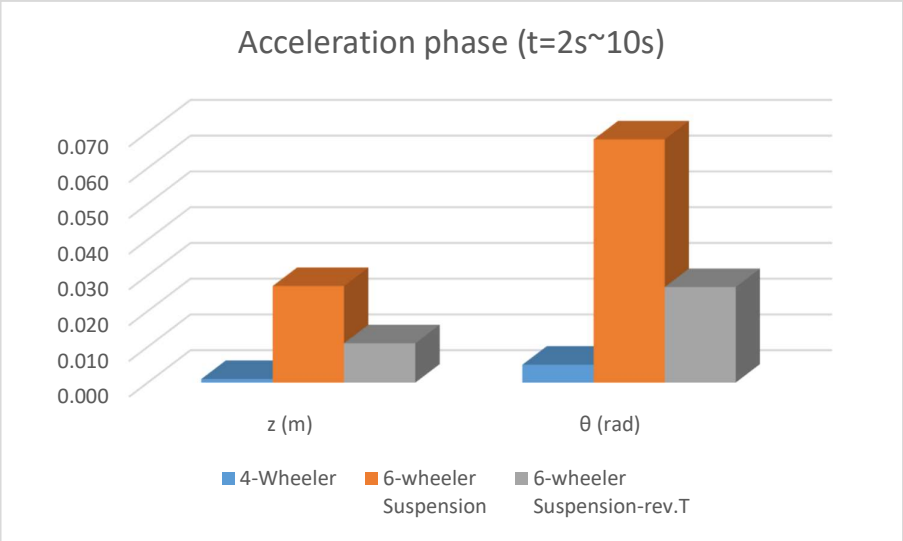

Figure 4.16 Comparison-Acceleration phase (4- vs. 6-wheeler)

Step phase comparison is shown in Figure 4.17. Unlike acceleration phase, 4-wheeler's performance is only slightly better than that of 6-wheeler with suspension during step phase.

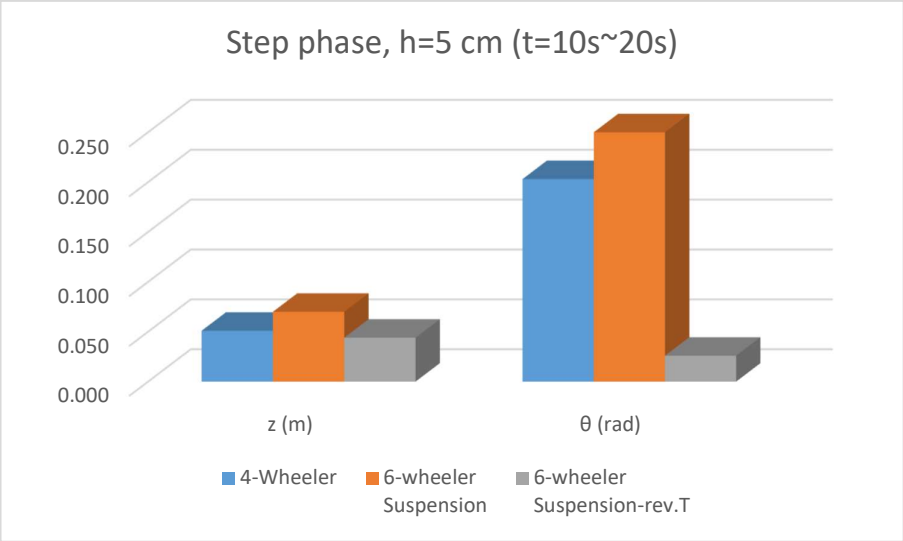

Figure 4.17 Comparison-Step phase (4- vs. 6-wheeler)

One reason could be found from the structure of 4-wheeler. The wheel leg being stretched out to the front and to the rear extending the moment arm of the vehicle body causes higher pitching torque. Also, torsional spring-damper systems for the front wheel and the rear wheel need to be tuned differently to reduce pitching. Assuming COM location to be in the middle of the body, slightly softer front wheel suspension and a stiffer rear wheel suspension could reduce pitching and make smoother entrance and settling on the step.

5. CONCLUSION

The study researched 6-wheel based and 4-wheel based ADR for LMD applications. Cruising stability including ground contact issues of 6-wheelers which are already operating in the market was depicted and novel design of 4-wheeler with curb climbing feature is introduced. Based on the equations of motions, the suspension dynamic models are created using MATLAB Simulink, and results were compared.

6-wheeler without suspension system is highly exposed to vibration and external disturbances. 6-wheeler with suspension model shows relatively smooth shock absorption ability but did not effectively narrow pitching and vertical displacement. Applying reverse torque helped reducing the gap but elevating the bogie will make the middle wheel lose its contact with the ground. Therefore, applying reverse torque should be limited to temporary function. In general, 6-wheeler has outstanding structural stability and a cute looking appearance. However, when it comes to cruising and ground contact, it has significant technical challenges.

To overcome and tackle such problems, 4-wheeler with 2 belly wheels is introduced. The vehicle has a symmetric structure having 4 identical independent wheel mechanism on each joint, which gives sound balance of the chassis.

A comparative study shows that 4-wheeler outperforms, especially during acceleration phase – Less than 10% vertical response and 20% pitching response than those of 6-wheeler with reverse torque. The study is expected to provide a novel concept of 4-wheeler ADR for LMD applications.

Future work for 4-wheeler will cover the following.

- Validation and efficacy of dummy roller without motor engagement.
- Dynamic modelling of COM deviations within the body to achieve stable manoeuvrability of the vehicle, especially during curb-climbing task.
- Parametric study on different design parameters such as dimensions, spring constant & damping coefficients etc.
- Building prototype for a field test.

SUMMARY

ADR for LMD applications is becoming more popular these days. 6-wheel ADR with a bogie mechanism has many benefits, including curb-climbing features. However, the 2-wheel inter-dependent bogie mechanism makes the intricate behaviour of rear wheel suspension result in unstable cruising and ground contact. To improve these problems, installing a shock-absorbing suspension system is considered. Due to the lack of space in the chassis, cantilever types for the front and torsional springs are proposed. To study cruising stability, a simulation model is created using MATLAB Simulink. A half-car suspension model is created based on spring-damper suspension dynamics.

In addition to the 6-wheeler, a novel design of the 4-wheeler with a double belly wheel is introduced. The technical features and inner mechanism layout are presented in the CAD model. The 4-wheeler can also climb curbs using stretchable wheel legs. A simulation model of suspension is also created for 4-wheelers.

Results for both models are compared under identical cruising environments with the same acceleration and step input. The results show that the 4-wheeler's vertical displacement response outperforms compared with that of the 6-wheeler suspension with reverse torque applied—a 90% decrease in vertical displacement and an over 80% decrease in angular displacement during the acceleration phase. On the other hand, 4-wheel suspension shows only a slight improvement compared with 6-wheel suspension without reverse torque applied.

[eesti keeles]

ADR on LMD-rakenduste puhul tänapäeval üha populaarsemaks muutumas. 6-rattalisel ADR-veokil on palju eeliseid, sealhulgas ka kõnniteele tõusmise funktsioonid. Kuid 2-rattaline, üksteisest sõltuv telkmehhanism muudab tagaratta vedrustuse keerulise käitumise, mille tulemuseks on ebastabiilne liikumine ja maapinnaga kokkupuutumine. Nende probleemide lahendamiseks kaalutakse löögisüsteemi paigaldamist. Ruumipuuduse tõttu šassiis tehakse ettepanek kasutada esiosa ja väändusvedrusid. Sõiduki stabiilsuse uurimiseks luuakse simulatsioonimudel MATLAB Simulinki abil. Luuakse poolauto vedrustuse mudel, mis põhineb vedru-amortisaatoriga vedrustuse dünaamikal.

Lisaks 6-veolisele rattale tutvustatakse ka uudset 4-veolise ratta konstruktsiooni, millel on kahekordne kõhveratas. Tehnilised omadused ja sisemine mehhanismi paigutus on esitatud CAD-mudeli abil. 4-ratas suudab ka kõnniteele ronida, kasutades venitatavaid rattajalgu. 4-ratturi jaoks on loodud ka vedrustuse simulatsioonimudel.

Mõlema mudeli tulemusi võrreldakse identsetes sõidukeskkondades - sama kiirendus ja samad sammud. Tulemused näitavad, et 4-ratturi vertikaalse nihke reaktsioon on parem

kui 6-ratturi vedrustuse reaktsioon, kui rakendatakse pöördemomenti - vertikaalse nihke vähenemine 90% ja nurknihke vähenemine üle 80% kiirendusfaasis. Teisest küljest on 4-rattalise vedrustuse puhul ainult väike paranemine võrreldes 6-rattalise vedrustusega ilma pöördmomendi rakendamiseta.

LIST OF REFERENCES

[1] S. Srinivas, S. Ramachandiran and S. Rajendran, "Autonomous robot-driven deliveries: A review of recent developments and future directions", Transp. Res. Part E Logist. Transp. Rev., vol 165, p 102834, 9 2022, doi: 10.1016/j.tre.2022.102834.

[2] "Starship Robot Dimensions & Drawings | Dimensions.com". qAccessed: 2024-3- 16. [Online]. Available at: https://www.dimensions.com/element/starship-robot

[3] E. Ayyildiz and M. Erdogan, "Addressing the challenges of using autonomous robots for last-mile delivery", Comput. Ind. Eng., vol 190, p 110096, 4 2024, doi: 10.1016/j.cie.2024.110096.

[4] J. Zhao et al., "Autonomous driving system: A comprehensive survey", Expert Syst. Appl., vol 242, p 122836, 5 2024, doi: 10.1016/j.eswa.2023.122836.

[5] J. Zhao et al., "Autonomous driving system: A comprehensive survey", Expert Syst. Appl., vol 242, p 122836, 5 2024, doi: 10.1016/j.eswa.2023.122836.

[6] D. Kim, H. Hong, H. S. Kim and J. Kim, "Optimal design and kinetic analysis of a stair-climbing mobile robot with rocker-bogie mechanism", Mech. Mach. Theory, vol 50, pp 90–108, 4 2012, doi: 10.1016/j.mechmachtheory.2011.11.013.

[7] H. Zhao, C. Luo, Y. Xu and J. Li, "Differential Steering Control for 6 × 6 Wheel-drive Mobile Robot", in 2021 26th International Conference on Automation and Computing (ICAC), Portsmouth, United Kingdom: IEEE, 9 2021, pp 1–6. doi: 10.23919/ICAC50006.2021.9594210.

[8] J. Nah, K. Yi, W. Kim and Y. Yoon, "Torque Distribution Algorithm of Six-Wheeled Skid-Steered Vehicles for On-Road and Off-Road Maneuverability", presented at the SAE 2013 World Congress & Exhibition, 4 2013, pp 2013-01–0628. doi: 10.4271/2013-01-0628.

[9] A. K. Gupta and V. K. Gupta, "Design and development of six-wheeled Multi-Terrain Robot", in 2013 International Conference on Control, Automation, Robotics and Embedded Systems (CARE), Jabalpur, India: IEEE, 12 2013, pp 1–6. doi: 10.1109/CARE.2013.6733751.

[10] Z. Song, Z. Luo, G. Wei and J. Shang, "A Portable Six-Wheeled Mobile Robot With Reconfigurable Body and Self-Adaptable Obstacle-Climbing Mechanisms", J. Mech. Robot., vol 14, 5, Art. 5, 10 2022, doi: 10.1115/1.4053529.

[11] V. Tavoosi, D. J. M. Rad and D. R. Mirzaei, "Vertical Dynamics Modeling and Simulation of a Six-Wheel Unmanned Ground Vehicle", p 21.

[12] J. M. Muñoz-Guijosa, D. Fernández Caballero, V. Rodríguez De La Cruz, J. L. Muñoz Sanz and J. Echávarri, "Generalized spiral torsion spring model", Mech. Mach. Theory, vol 51, pp 110–130, 5 2012, doi: 10.1016/j.mechmachtheory.2011.12.007.

[13] B. T. Knox and J. P. Schmiedeler, "A Unidirectional Series-Elastic Actuator Design Using a Spiral Torsion Spring", J. Mech. Des., vol 131, 12, Art. 12, 12 2009, doi: 10.1115/1.4000252.

[14] S. Rossi, F. Patane, F. Del Sette and P. Cappa, "WAKE-up: A wearable ankle knee exoskeleton", in 5th IEEE RAS/EMBS International Conference on Biomedical Robotics and Biomechatronics, Sao Paulo, Brazil: IEEE, 8 2014, pp 504–507. doi: 10.1109/BIOROB.2014.6913827.

[15] W. M. dos Santos, G. A. P. Caurin and A. A. G. Siqueira, "Design and control of an active knee orthosis driven by a rotary Series Elastic Actuator", Control Eng. Pract., vol 58, pp 307–318, 1 2017, doi: 10.1016/j.conengprac.2015.09.008.

[16] J. Ju, Y. Zhao, C. Zhang and Y. Liu, "Vibration Suppression of a Flexible-Joint Robot Based on Parameter Identification and Fuzzy PID Control", Algorithms, vol 11, 11, Art. 11, 11 2018, doi: 10.3390/a11110189.

[17] D. Campolo, M. Azhar, G.-K. Lau and M. Sitti, "Can DC Motors Directly Drive Flapping Wings at High Frequency and Large Wing Strokes?", IEEEASME Trans. Mechatron., vol 19, 1, Art. 1, 2 2014, doi: 10.1109/TMECH.2012.2222432.

[18] B. Joshi, R. Shrestha and R. Chaudhary, "Modeling, Simulation and Implementation of Brushed DC Motor Speed Control Using Optical Incremental Encoder Feedback", p 9, 2014.

[19] W. Homik and P. Grzybowski, "The simulation model of small-dimension rubbery torsional vibration damper", . ISSN, vol 6, 2015.

[20] S. Shahjahan Ahmad et al., "Torque Limiters for Aerospace Actuator Application", Energies, vol 15, 4, p 1467, 2 2022, doi: 10.3390/en15041467.

[21] "Ball Detent Torque Limiter: Overload Clutch", Ball Detent Torque Limiter. Accessed: 2024- 5- 10. [Online]. Available at: https://mechanical-design-handbook.blogspot.com/2012/05/ball-detent-torque-limiter-overload.html

[22] "Different Types of Motors Used In Robotics", Robocraze. Accessed: 2024- 3- 18. [Online]. Available at: https://robocraze.com/blogs/post/types-of-motors-used-in-robotics

[23] "Servo Motors Advantages and Disadvantages - RealPars". Accessed: 2024- 3- 18. [Online]. Available at: https://www.realpars.com/blog/servo-motors-advantages

[24] "Stepper Motors Advantages and Disadvantages - RealPars". Accessed: 2024- 3- 18. [Online]. Available at: https://www.realpars.com/blog/stepper-motors-advantages

[25] S.-H. Kim, "Fundamentals of electric motors", in Electric Motor Control, Elsevier, 2017, pp 1–37. doi: 10.1016/B978-0-12-812138-2.00001-5.

[26] Y. Deng, Z. Wang, H. Shen, J. Gong and Z. Xiao, "A comprehensive review on non-pneumatic tyre research", Mater. Des., vol 227, p 111742, 3 2023, doi: 10.1016/j.matdes.2023.111742.

[27] Y. Luet al., "From nano to giant? Designing carbon nanotubes for rubber reinforcement and their applications for high performance tires", Compos. Sci. Technol., vol 137, pp 94–101, 12 2016, doi: 10.1016/j.compscitech.2016.10.020.

[28] G. K. Awari, V. S. Kumbhar and R. B. Tirpude, Automotive systems: principles and practice, First edition. Boca Raton London New York: CRC Press, Taylor & Francis Group, 2021.

[29] "Moment of inertia - Steiner's theorem".

[30] "13.8: Parallel-Axis Theorem", Physics LibreTexts. Accessed: 2024- 5- 12. [Online]. Available at: https://phys.libretexts.org/Bookshelves/Classical_Mechanics/Variational_Principles_in_Classical_Mechanics_(Cline)/13%3A_Rigid-body_Rotation/13.08%3A_Parallel-Axis_Theorem

[31] "Parallel Axis Theorem: Definition, Formula, Proof & Example", StudySmarter UK. Accessed: 2024- 5- 12. [Online]. Available at: https://www.studysmarter.co.uk/explanations/physics/classical-mechanics/parallel-axis-theorem/